



**HAL**  
open science

## Hepatitis C virus (HCV) protein expression enhances hepatic fibrosis in HCV transgenic mice exposed to a fibrogenic agent.

Philippe Chouteau, Nicole Defer, Alexandre Florimond, Julien Caldéraro, Martin Higgs, Aurore Gaudin, Emilie Mérour, Daniel Dhumeaux, Hervé Lerat, Jean-Michel Pawlotsky

### ► To cite this version:

Philippe Chouteau, Nicole Defer, Alexandre Florimond, Julien Caldéraro, Martin Higgs, et al.. Hepatitis C virus (HCV) protein expression enhances hepatic fibrosis in HCV transgenic mice exposed to a fibrogenic agent.. *Journal of Hepatology*, 2012, 57 (3), pp.499-507. 10.1016/j.jhep.2012.04.019 . inserm-00734273

**HAL Id: inserm-00734273**

**<https://inserm.hal.science/inserm-00734273>**

Submitted on 21 Sep 2012

**HAL** is a multi-disciplinary open access archive for the deposit and dissemination of scientific research documents, whether they are published or not. The documents may come from teaching and research institutions in France or abroad, or from public or private research centers.

L'archive ouverte pluridisciplinaire **HAL**, est destinée au dépôt et à la diffusion de documents scientifiques de niveau recherche, publiés ou non, émanant des établissements d'enseignement et de recherche français ou étrangers, des laboratoires publics ou privés.

1  
2  
3  
4 **Hepatitis C Virus (HCV) Protein Expression Enhances Hepatic Fibrosis**  
5  
6  
7 **in HCV Transgenic Mice Exposed to a Fibrogenic Agent**  
8  
9

10  
11  
12 Philippe Chouteau,<sup>1,2</sup> Nicole Defer,<sup>1</sup> Alexandre Florimond,<sup>1,2</sup> Julien Caldéraro,<sup>2,3</sup>  
13  
14 Martin Higgs,<sup>1‡</sup> Aurore Gaudin,<sup>1</sup> Emilie Mérour,<sup>1</sup> Daniel Dhumeaux,<sup>1,2</sup> Hervé Lerat,<sup>1,2</sup>  
15  
16  
17 and Jean-Michel Pawlotsky<sup>1,2,4</sup>  
18  
19  
20  
21

22 <sup>1</sup>Inserm U955, Créteil, France ; <sup>2</sup>Université Paris-Est, Créteil, France;

23  
24 <sup>3</sup>Department of Pathology, Hôpital Henri Mondor, Créteil, France, <sup>4</sup>National  
25  
26  
27 Reference Center for Viral Hepatitis B, C, and Delta, Department of Virology,  
28  
29  
30 Hôpital Henri Mondor, Créteil, France  
31

32  
33  
34 <sup>‡</sup>Present address : Cancer Research UK Institute for Cancer Sciences,  
35  
36  
37 University of Birmingham, Birmingham, B15 2TT, UK  
38  
39  
40  
41  
42  
43

44 **Corresponding Author:** Prof. , MD, PhD, Department of Virology, Hôpital Henri  
45  
46 Mondor, 51 avenue du Maréchal de Lattre de Tassigny, 94010 Créteil, France.

47  
48  
49 Tel: +33-1-4981-2827 ; Fax: +33-1-4981-4831  
50

51  
52 E-mail: jean-michel.pawlotsky@hmn.aphp.fr  
53  
54  
55

56  
57 **Electronic word count:** 5946  
58

59 **Abstract electronic word count:** 244  
60  
61  
62  
63  
64  
65

1  
2  
3  
4 **Number of figures:** [6](#)

5  
6  
7 **Number of tables:** 1

8  
9  
10  
11 **List of abbreviations:** HCV, hepatitis C virus; ORF, open reading frame; ECM, extra-  
12 cellular matrix; CCl<sub>4</sub>, carbon tetrachloride; wt, wild-type; qPCR, quantitative PCR;  
13  
14 hepatic stellate cells; HPCs, hepatic progenitor cells; PBS, phosphate buffer saline;  
15  
16 CYP2E1, cytochrome P450 2E1; ROS, reactive oxygen species; BrdU,  
17  
18 bromodeoxyuridine; ALT, alanine aminotransferase; AST, aspartate aminotransferase;  
19  
20  
21  
22  
23  
24 CCL5, chemokine (C-C motif) ligand 5.

25  
26  
27  
28 **Conflict of interest:** The authors declare that they have nothing to disclose regarding  
29  
30  
31  
32  
33  
34  
35  
36  
37  
38  
39  
40  
41  
42  
43  
44  
45  
46  
47  
48  
49  
50  
51  
52  
53  
54  
55  
56  
57  
58  
59  
60  
61  
62  
63  
64  
65  
conflict of interest with respect to this manuscript.

66  
67  
68  
69  
70  
71  
72  
73  
74  
75  
76  
77  
78  
79  
80  
81  
82  
83  
84  
85  
86  
87  
88  
89  
90  
91  
92  
93  
94  
95  
96  
97  
98  
99  
100  
**Financial Support:** This study was supported by the National Agency for Research on  
AIDS and Viral Hepatitis (ANRS; R0711JJ and R09017JJ). A. F. is the recipient of a  
postdoctoral fellowship from the French Ministry of Research; M. H. was the recipient of  
a postdoctoral fellowship from the ANRS.

## ABSTRACT

**Background & Aims:** During chronic HCV infection, activation of fibrogenesis appears to be principally related to local inflammation. However, the direct role of hepatic HCV protein expression in fibrogenesis remains unknown.

**Methods:** We used transgenic mice expressing the full-length HCV open reading frame exposed to a 'second hit' of the fibrogenic agent carbon tetrachloride (CCl<sub>4</sub>). Both acute and chronic liver injuries were induced in these mice by CCl<sub>4</sub> injections. Liver injury, expression of matrix re-modeling genes, reactive oxygen species (ROS), inflammation, hepatocyte proliferation, ductular reaction and hepatic progenitor cells (HPC) expansion were examined.

**Results:** After CCl<sub>4</sub> treatment, HCV transgenic mice exhibited enhanced liver fibrosis, significant changes in matrix re-modeling genes and increased ROS production compared to wt littermates despite no differences in the degree of local inflammation. This increase was accompanied by a decrease in hepatocyte proliferation, which appeared to be due to delayed hepatocyte entry into the S-phase. A prominent ductular reaction and hepatic progenitor cell compartment expansion were observed in transgenic animals. These observations closely mirror those previously made in HCV-infected individuals.

**Conclusions:** Together, these results demonstrate that expression of the HCV proteins in hepatocytes contributes to the development of hepatic fibrosis in the presence of other fibrogenic agents. In the presence of CCl<sub>4</sub>, HCV transgenic mice display an intra-hepatic re-organization of several key cellular actors in the fibrogenic process.

1  
2  
3  
4  
5  
6 **Keywords:** hepatitis C virus; fibrosis; hepatocyte proliferation; reactive oxygen species;  
7  
8 ductular reaction; hepatic progenitor cells  
9  
10  
11  
12  
13  
14  
15  
16  
17  
18  
19  
20  
21  
22  
23  
24  
25  
26  
27  
28  
29  
30  
31  
32  
33  
34  
35  
36  
37  
38  
39  
40  
41  
42  
43  
44  
45  
46  
47  
48  
49  
50  
51  
52  
53  
54  
55  
56  
57  
58  
59  
60  
61  
62  
63  
64  
65

## INTRODUCTION

Hepatic fibrosis, a result of active fibrogenesis, is a frequent feature of chronic hepatitis C virus (HCV) infection. Fibrogenesis is classically thought to be triggered principally by the local immune response. The role of HCV infection in fibrogenesis, in particular HCV protein expression in the liver, is unknown. Mice of the FL-N/35 lineage express the entire open reading frame (ORF) of a genotype 1b isolate of HCV in a liver-specific fashion [1]. In this model, the HCV proteins are expressed within hepatocytes at levels close to those observed in human infection, without infectious virus production or an antiviral immune response. These mice develop lesions similar to those observed during natural infection, including hepatic steatosis and hepatocellular carcinoma [2-6]. Preliminary observations suggested that FL-N/35 mice may be of interest in the study of liver fibrosis [1]. However, this model lacks the concomitant fibrogenesis triggers (such as liver inflammation) observed in HCV-infected individuals. Therefore, the effect of HCV protein expression on hepatic fibrosis in this model must be studied in the context of a 'second hit' of chronic liver injury.

The conventional paradigm of fibrogenesis in the liver is largely based on activation of fibrogenic processes associated with transformation of hepatic stellate cells (HSCs) into myofibroblast-like cells [7-10]. However, it remains paradoxical that, whereas HCV infection is present largely within hepatic lobules [11], fibrosis predominates in portal areas in chronically infected patients. Currently, there are no explanations for this observation, and the surrounding mechanisms remain

1  
2  
3  
4 uninvestigated. One possible explanation is that viral particles produced within  
5  
6 intralobular hepatocytes might directly activate periportal HSCs. Another non-exclusive  
7  
8 explanation is that HCV infection may be accompanied by ductular proliferation [12].  
9

10  
11 In the normal liver, the replacement of necrotic and apoptotic hepatocytes occurs  
12  
13 through replication of adjacent hepatocytes within the lobules. However, this primary  
14  
15 pathway is impaired by a variety of insults, including viral infections [13, 14]. These  
16  
17 situations have been shown to lead to proliferation of hepatic progenitor cells (HPCs)  
18  
19 [15-17]. Such cells reside primarily in the periportal region and become the source of  
20  
21 regenerating hepatocytes, as well as cholangiocytes and draining ductules [15, 18]. A  
22  
23 by-product of the activation of this secondary proliferative pathway is a ductular reaction  
24  
25  
26  
27  
28 [15], which has been linked to fibrogenesis [19-28].  
29

30  
31 A strong correlation has been reported between HCV-related portal fibrosis and a  
32  
33 periportal ductular reaction, with a relationship between the number of proliferating  
34  
35 HPCs and the number of hepatocytes in replication arrest [29]. These observations  
36  
37 support the hypothesis that portal fibrosis during chronic HCV infection may result from  
38  
39 a periportal ductular reaction, possibly as a consequence of altered hepatocyte  
40  
41 proliferation, possibly as a consequence of altered hepatocyte  
42  
43 proliferation.  
44

45  
46 We illustrate below, using the FL-N/35 HCV transgenic mouse model in  
47  
48 conjunction with an exogenous chemical fibrogenic agent, that the expression of HCV  
49  
50 proteins *in vivo* plays a contributory role in the fibrogenic process, and is accompanied  
51  
52 by a ductular reaction and a replicative arrest of intra-lobular hepatocytes concomitant  
53  
54 with enhanced reactive oxygen species (ROS) production, in the absence of enhanced  
55  
56 inflammation.  
57  
58  
59  
60  
61  
62  
63  
64  
65

## MATERIALS AND METHODS

### *Chemicals and antibodies*

Carbon tetrachloride (CCl<sub>4</sub>) and olive oil were purchased from Sigma-Aldrich (St. Louis, MO). Primary antibodies are described in more details in Supplementary Materials and Methods.

### *Animals*

Wild-type mice (wt) and those transgenic for the entire HCV ORF (FL-N/35 lineage) were from the same genetic background (C57/Bl6) [1]. They were used in conformation with the European Community Council directive. Animals were bred and housed as previously described [2]. Studies were performed on age-matched 7- to 10-month old males.

### *Chronic CCl<sub>4</sub> treatment*

Animals were injected intraperitoneally twice a week for 4 weeks with CCl<sub>4</sub> (0.5 μg/g of body weight) diluted in 5% olive oil, obtained the day of injection. Control mice were injected with an equal volume of olive oil. Twenty-four hours after the final injection, animals were sacrificed by CO<sub>2</sub> inhalation, and body and liver weights were measured. Sera (100 μL/mouse) and livers were immediately processed for enzymatic

assays and histological determination, or kept at -80 °C until processing.

### **Experimental acute liver injury and measurement of hepatocyte DNA**

#### **synthesis**

Mice were treated with a single intraperitoneal injection of CCl<sub>4</sub> (795 mg/kg body weight diluted in 5% olive oil). They were sacrificed at different time points after the injection. Bromodeoxyuridine (BrdU) was injected intraperitoneally (150 mg/kg of body weight) two hours prior to sacrifice. Hepatocyte DNA synthesis was measured by means of immunodetection of BrdU incorporation as described in Supplementary Materials and Methods.

#### ***Western blotting***

Frozen liver tissues were processed as previously described [6]. The detailed procedure is described in Supplementary Materials and Methods.

#### ***Serum alanine aminotransferase and aspartate aminotransferase level measurements***

Levels of alanine aminotransferase (ALT) and aspartate aminotransferase (AST) in the serum of mice were measured on a Cobas<sup>®</sup>6000 analyzer (Roche, Diagnostics, Basel, Switzerland), according to the manufacturer's instructions.

### ***Liver histology and immunohistochemistry***

Fresh liver tissues were fixed in 10% buffered formalin, paraffin-embedded, and 5  $\mu\text{m}$  sections were prepared. Standard histology and immunostainings are described in Supplementary Materials and Methods.

### ***Quantification of hepatocyte reactive oxygen species (ROS)***

Frozen liver sections (10  $\mu\text{m}$ ) from wt and FL-N/35 mice were assessed for the presence of ROS, as previously described [4]. The percentage of ROS-specific hepatocytes was calculated, and normalized to that in wt controls. In all cases (CCl<sub>4</sub>-treated and untreated mice), only large cells with round nuclei present within the parenchyma were considered as hepatocytes.

### ***RNA isolation and quantitative real-time PCR analysis***

Total RNA and complementary DNA were purified and synthesized, respectively, as previously described [6]. Quantitative PCR was performed with an Applied Biosystems 7300 Thermal Cycler using Taqman reagents (Applied Biosystems), as described in Supplementary Materials and Methods.

### ***Measurement of CCL5 protein in liver tissues***

1  
2  
3  
4 CCL5 protein was quantified in frozen liver tissues according to the procedure  
5  
6 described in Supplementary Materials and Methods.  
7  
8  
9

### 10 11 ***Image analysis*** 12 13

14  
15  
16 Tissue sections were photographed using a Zeiss Axioskop 40 microscope in  
17  
18 conjunction with a Zeiss MRc5 Axiocam and Axiovision LE software (Zeiss, Jena,  
19  
20 Germany). Image analyses were performed as described in Supplementary Materials  
21  
22 and Methods.  
23  
24  
25

### 26 27 28 ***Statistical analyses*** 29 30 31

32  
33 Statistical analyses were performed using Prism software (GraphPad Software  
34  
35 Inc., La Jolla, CA). Results are expressed as mean±standard error of the mean (SEM).  
36  
37 Box-and-whisker graphs are used; the line in the middle is the median, the box extends  
38  
39 from the 25th to the 75th percentile, and the whiskers extend to the lowest and highest  
40  
41 values. To determine the statistical significance of the data, Mann-Whitney non-  
42  
43 parametrical tests were performed. Pearson's correlation coefficient was used to  
44  
45 determine correlations between continuous normally distributed variables. All *P* values  
46  
47 were two-tailed, with *P* values less than 0.05 considered as significant.  
48  
49  
50  
51  
52  
53  
54  
55  
56  
57  
58  
59  
60  
61  
62  
63  
64  
65

## RESULTS

### ***Hepatic expression of the full-length HCV ORF enhances liver fibrosis induced by CCl<sub>4</sub> in HCV transgenic mice***

The extent of extracellular matrix (ECM) deposition occurring within the liver of wt and FL-N/35 mice chronically exposed to CCl<sub>4</sub> was determined by picosirius red staining of formalin-fixed, paraffin-embedded liver sections. As shown in Fig. 1A and 1B, ECM deposition was observed only in normal anatomical structures such as portal tracts in untreated FL-N/35 and wt mice. Thus, in the absence of an exogenous fibrogenic stimulus, expression of the HCV proteins does not *per se* stimulate ECM deposition at a level detectable using picosirius staining.

In CCl<sub>4</sub>-treated wt and FL-N/35 animals, picosirius red staining demonstrated established fibrosis with distinctive septa-like morphologies (Fig. 1A and 1B). In both transgenic and nontransgenic animals, the quantity of ECM was significantly greater than in the corresponding untreated animals (Fig. 1B). In CCl<sub>4</sub>-treated mice, the quantity of ECM was significantly greater in FL-N/35 than in wt animals (median collagen deposition: 1.7, range 1.0-2.8 vs 1.2, range, 0.9-2.4;  $P=0.0039$ ) (Fig. 1B).

As differences in the expression of cytochrome P450 2E1 (CYP2E1), the enzyme responsible for bioactivation of CCl<sub>4</sub>, could be responsible for the observed difference [30], we quantified CYP2E1 expression by western blotting in HCV transgenic and wt animals. No difference was found between the two groups (Supplementary Fig. S1).

Overall, these results suggest that intrahepatic expression of the HCV proteins *in vivo* potentiates the fibrogenic effect of the exogenous agent CCl<sub>4</sub>.

1  
2  
3  
4  
5  
6  
7 ***Increased liver fibrosis induced by CCl<sub>4</sub> in transgenic mice is not due to a***  
8  
9 ***higher degree of necroinflammation in the presence of HCV proteins***  
10

11  
12  
13  
14 We examined the role of HCV protein expression in liver necroinflammation in the  
15 presence and absence of CCl<sub>4</sub>. Hematoxylin-eosin staining of liver tissues showed  
16 normal hepatic architecture in wt and FL-N/35 mice that did not receive CCl<sub>4</sub>  
17 (Supplementary Fig. S2). In contrast, CCl<sub>4</sub>-treated animals showed remnants of  
18 degenerated and ballooned/necrotic hepatocytes, equivalently present in wt and FL-  
19 N/35 mice. Mild mononuclear cell infiltration in the same areas was also evenly present  
20 in these animals.  
21  
22  
23  
24  
25  
26  
27  
28  
29

30  
31 Expression of F4/80 mRNA, a marker of resident and recruited macrophages, did  
32 not differ between untreated wt and FL-N/35 animals. F4/80 mRNA expression was  
33 induced to the same degree in both transgenic and non-transgenic mice after chronic  
34 CCl<sub>4</sub> administration (Supplementary Fig. S3). Immunostaining of liver tissues with the  
35 pan-T lymphocyte marker CD3 revealed similar degrees of T lymphocyte infiltration in wt  
36 and FL-N/35 mice exposed to CCl<sub>4</sub>, with CD3-positive cells present along hepatic septa  
37 (Supplementary Fig. S4).  
38  
39  
40  
41  
42  
43  
44  
45  
46  
47

48 The chemokine CCL5 is secreted by T-cells and macrophages and could play a  
49 role in fibrosis by stimulating hepatic stellate cells [31]. CCL5 expression did not differ  
50 between wt and FL-N/35 animals, both in the presence and absence of CCl<sub>4</sub>  
51 (Supplementary Figs. S5 and S6).  
52  
53  
54  
55  
56

57 Taken together, these results suggest that enhanced fibrosis in HCV-transgenic  
58 mice exposed to CCl<sub>4</sub> is not mediated by an increased necroinflammation.  
59  
60  
61  
62  
63  
64  
65

1  
2  
3  
4  
5  
6  
7 **Increased liver fibrosis induced by CCl<sub>4</sub> in transgenic mice is associated**  
8  
9 **with alterations in the expression of genes involved in ECM remodeling**

10  
11  
12  
13  
14 We measured the hepatic expression of a number of ECM remodeling genes,  
15 including genes coding for ECM components (collagens), proteins involved in ECM  
16 production/degradation (matrix metalloproteinases [MMP]) and regulators of MMPs  
17 (tissue inhibitors of metalloproteinase [TIMP]) in the different groups of mice. As shown  
18 in Fig. 2, in the absence of an exogenous fibrogenic stimulus, the expression of HCV  
19 proteins in hepatocytes was not associated with higher levels of expression of these  
20 genes. In CCl<sub>4</sub>-treated wt animals, expression of all of the tested mRNA levels was  
21 significantly modified compared to the untreated mice, but in various directions (Fig. 2).  
22  
23 Among the different collagen genes tested, only collagen 1 $\alpha$ 1 expression was notably  
24 enhanced in FL-N/35 compared to wt CCl<sub>4</sub>-treated mice, although the results did not  
25 reach statistical significance (p = 0,055). The expression of the other collagens showed  
26 no difference (Fig. 2A). MMP7 mRNA levels were significantly lower in HCV transgenic  
27 than in non-transgenic CCl<sub>4</sub>-treated animals, whereas the expression of MMP13, MMP3  
28 and TIMP1 was notably but not significantly lower (p values between 0.052 and 0.055,  
29 Fig. 2B and 2C). These results were in keeping with the increase in ECM deposition  
30 observed in HCV transgenic animals treated with CCl<sub>4</sub>.

31  
32  
33  
34  
35  
36  
37  
38  
39  
40  
41  
42  
43  
44  
45  
46  
47  
48  
49  
50  
51  
52  
53  
54  
55 ***Liver fibrosis is associated with decreased hepatocyte proliferation in HCV***  
56 ***transgenic mice chronically exposed to CCl<sub>4</sub>***  
57  
58  
59  
60  
61  
62  
63  
64  
65

1  
2  
3  
4  
5  
6  
7 Since hepatic fibrosis in HCV-infected patients has been associated with  
8 increased hepatocyte replicative arrest [29], we next examined the extent of hepatocyte  
9 proliferation in wt and FL-N/35 mice in the presence and absence of CCl<sub>4</sub>. Hepatocyte  
10 proliferation was evaluated by immunohistochemistry for Ki67, a nuclear antigen that is  
11 expressed in G1, S, G2 and M phases of the cell cycle, but absent in G0 or quiescent  
12 phase. In the absence of chronic CCl<sub>4</sub> exposure, a very low proportion of proliferative  
13 hepatocytes was observed in both wt and FL-N/35 mice, with no differences between  
14 these two groups, suggesting low-level basal renewal of the mature hepatocyte pool in  
15 the parenchyma (Fig. 3A and 3B).  
16  
17  
18  
19  
20  
21  
22  
23  
24  
25  
26  
27

28 As a consequence of chronic exposure to CCl<sub>4</sub>, hepatocyte proliferation was  
29 significantly increased in both wt and FL-N/35 mice compared to non-exposed animals  
30 (Fig. 3A and 3B). As shown in Fig. 3B, hepatocyte proliferation was significantly lower in  
31 CCl<sub>4</sub>-exposed FL-N/35 than in wt mice (median positive hepatocytes, 25.1 %, range 7.1-  
32 65.7 %, vs 30.3 %, range 5.9-49.2 %, respectively;  $P=0.002$ ). No difference in the  
33 distribution of proliferating hepatocytes within the parenchyma was observed between  
34 treated wt and FL-N/35 animals.  
35  
36  
37  
38  
39  
40  
41  
42  
43  
44

45 In HCV-transgenic mice exposed to CCl<sub>4</sub>, a significant inverse relationship  
46 between the number of Ki67 positive hepatocytes and the extent of ECM deposition was  
47 observed ( $r=0.893$ ,  $P=0.012$ ; Fig. 3C). In contrast, no correlation was found in CCl<sub>4</sub>-  
48 exposed wt mice ( $r=0.1022$ ,  $P=0.81$ ; Fig. 3D).  
49  
50  
51  
52  
53  
54

55 In concert, these results suggest that fibrosis induced by CCl<sub>4</sub> exposure in the  
56 context of HCV protein expression is concomitant with a lowered capability of  
57 hepatocytes to regenerate.  
58  
59  
60  
61  
62  
63  
64  
65

1  
2  
3  
4  
5  
6  
7 ***A prominent ductular reaction is present in HCV transgenic mice***  
8  
9 ***chronically exposed to CCl<sub>4</sub>***  
10

11  
12  
13  
14 Since decreased hepatocyte proliferation has been linked with the development  
15 of a ductular reaction in several hepatic disorders, in particular in HCV infection [29, 32],  
16 we next studied the ductular reaction in both wt and FL-N/35 mice by immunochemistry  
17 for cytokeratin 19 (CK19), a common bile duct, ductular epithelium and HPC marker in  
18 murine tissues. CK19-positive staining was limited to bile duct cholangiocytes in  
19 untreated wt and FL-N/35 mice, with no differences between the two groups (Fig. 4A  
20 and 4B).  
21  
22  
23  
24  
25  
26  
27  
28  
29

30  
31 Exposure of wt animals to CCl<sub>4</sub> did not modify the quantity and distribution of  
32 CK19-positive biliary epithelium (Fig. 4A and 4B). In contrast, HCV transgenic animals  
33 chronically exposed to CCl<sub>4</sub> presented a prominent positive staining for CK19,  
34 distributed at the periphery of the portal areas, in chords, clumps and rings, quite distinct  
35 from the anatomical bile ducts (Fig. 4A). The area occupied by CK19-positive biliary  
36 epithelium, comprising both anatomical bile ducts and the ductular reaction, was  
37 increased nearly 3-fold compared with CCl<sub>4</sub>-exposed wt mice (0.59% and 0.18%  
38 respectively,  $P=0.0016$ ; Fig. 4B).  
39  
40  
41  
42  
43  
44  
45  
46  
47  
48  
49

50 Altogether, these results suggest that fibrosis induced by CCl<sub>4</sub> exposure in the  
51 context of HCV protein expression is concomitant with a ductular reaction, which is  
52 absent in similarly treated wt animals.  
53  
54  
55  
56  
57  
58  
59  
60  
61  
62  
63  
64  
65

1  
2  
3  
4       ***The ductular reaction is associated with expansion of the HPC population in***  
5  
6  
7       ***HCV transgenic mice chronically exposed to CCl<sub>4</sub>***  
8  
9

10  
11       Since hepatic fibrosis in HCV-infected patients has been associated with  
12 increased HPC expansion [29], we assessed whether the increased ductular reaction  
13 was associated with expansion of the HPC population in HCV transgenic animals  
14 exposed to CCl<sub>4</sub>. HPCs were distinguished from cholangiocytes as being CK19-positive  
15 cells distal to sites of ductular reaction and isolated within the parenchyma, without the  
16 cord-like arrangement of the ductules. In the absence of CCl<sub>4</sub>, a few HPCs were visible  
17 in the livers from either wt or FL-N/35 mice (Fig. 4A and 4C). After chronic CCl<sub>4</sub>  
18 treatment, a non-significant trend towards a higher number of isolated CK19-positive  
19 cells than in the untreated animals was observed in wt mice (Fig. 4A and 4C). In CCl<sub>4</sub>-  
20 treated FL-N/35 mice, a statistically significant increase in CK19-positive cells was  
21 observed when compared to CCl<sub>4</sub>-treated wt mice ( $P=0.0016$ ; Fig. 4C).  
22  
23  
24  
25  
26  
27  
28  
29  
30  
31  
32  
33  
34  
35  
36  
37

38       We observed significant correlations between the number of HPCs per portal tract  
39 and the extent of ECM deposition ( $r=0.71$ ,  $P=0.0062$ ; Fig. 4D), and between the number  
40 of HPCs and the surface of the ductular reaction ( $r=0.7984$ ,  $P=0.0011$ ; Fig. 4E), which  
41 were independent of HCV protein expression. However, FL-N/35 animals displayed  
42 increased ECM deposition, an increased number of HPCs per portal tract, and a larger  
43 ductular reaction when compared with wt animals, suggesting that the viral proteins may  
44 exacerbate these phenomena.  
45  
46  
47  
48  
49  
50  
51  
52  
53  
54

55       Together, these data indicate that the increased ductular reaction observed in  
56 HCV transgenic mice is associated with expansion of the HPC population.  
57  
58  
59  
60  
61  
62  
63  
64  
65

1  
2  
3  
4       ***The expansion of the HPC population leads to normal liver reconstitution in***  
5  
6  
7       ***HCV transgenic mice chronically exposed to CCl<sub>4</sub>***  
8  
9

10  
11       As shown in Table 1, despite the decreased hepatocyte proliferation in FL-N/35  
12 transgenic mice chronically exposed to CCl<sub>4</sub> shown in Figs. 3A and 3B, no difference  
13 was observed in body or liver weights between olive oil- and CCl<sub>4</sub>-treated animals in  
14 both wt and FL-N/35 groups, suggesting that liver tissue reconstitution is not  
15 substantially impaired in HCV transgenic mice.  
16  
17  
18  
19  
20  
21  
22

23  
24  
25  
26       ***Hepatocyte cell cycle progression is impaired after acute liver injury in HCV***  
27  
28       ***transgenic mice***  
29  
30

31  
32  
33       In order to assess whether HCV protein expression impairs liver regeneration,  
34 hepatocyte proliferation was measured in both wt and FL-N/35 mice during the course of  
35 acute CCl<sub>4</sub>-induced liver injury (Fig. 5A). Analysis of BrdU incorporation showed no or  
36 very few BrdU-positive cells in wt and HCV transgenic mouse livers before CCl<sub>4</sub> injection  
37 (0h), indicating that the majority of liver cells were quiescent in G<sub>0</sub>. As shown in Fig. 5A  
38 and 5B, both wt and HCV transgenic animals showed a significant increase of BrdU-  
39 positive hepatocytes after CCl<sub>4</sub> injection, suggesting entry into the S-phase of the cell  
40 cycle. However, this phenomenon was delayed in HCV transgenic animals, with a peak  
41 of BrdU incorporation reached at 48 hours post-injection, compared to 40 hours post-  
42 injection in wt animals (Fig. 5B). These findings indicate that HCV protein expression is  
43 associated with a delay in early cell cycle progression after acute liver injury.  
44  
45  
46  
47  
48  
49  
50  
51  
52  
53  
54  
55  
56  
57  
58  
59  
60  
61  
62  
63  
64  
65

1  
2  
3  
4 **ROS production is enhanced in HCV transgenic mice treated or not with**  
5  
6 **CCl<sub>4</sub>**  
7  
8  
9

10  
11 Since oxidative stress has been reported to modulate the fibrogenic response and  
12 elevated ROS production is frequently observed in HCV infected cells [33, 34], we  
13 measured ROS levels in the livers of wt and FL-N/35 mice. Using dihydroethidium (DHE)  
14 as a marker for intracellular ROS, we found that hepatocyte-specific ROS levels were  
15 significantly higher in frozen liver sections from HCV transgenic mice compared to their  
16 wt littermates in the absence of CCl<sub>4</sub> treatment (Fig. 6A, upper panels and Fig. 6B). In  
17 CCl<sub>4</sub>-treated animals, ROS levels were significantly higher than in untreated animals in  
18 both the wt and FL-N/35 groups (Fig. 6A, lower panels), principally due to infiltrating  
19 cells. However, when ROS production was measured only in hepatocytes, the levels  
20 were significantly higher in CCl<sub>4</sub>-exposed FL-N/35 mice than in their wt counterpart  
21 animals (Fig. 6A, lower panels and Fig. 6B). These results show that intrahepatic  
22 expression of the HCV proteins is associated with enhanced baseline ROS levels and  
23 that this phenomenon is amplified by CCl<sub>4</sub> treatment.  
24  
25  
26  
27  
28  
29  
30  
31  
32  
33  
34  
35  
36  
37  
38  
39  
40  
41  
42  
43  
44

45 **DISCUSSION**  
46  
47  
48  
49

50 Several *in vitro* reports have suggested that HCV proteins can directly induce  
51 fibrogenetic processes. For example, it has been shown that the culture medium of  
52 Huh7 cells harboring the HCV subgenomic replicon is able to activate *in vitro*-cultured  
53 HSCs, demonstrating that virus production is not a pre-requisite for such activation [35].  
54  
55 Moreover, the core and nonstructural 5A (NS5A) proteins have been suggested to play  
56  
57  
58  
59  
60  
61  
62  
63  
64  
65

1  
2  
3  
4 a direct role in the alteration of the hepatocyte metabolism, partly *via* mitochondrial  
5  
6 deregulation which generates ROS, strong inducers of pro-fibrogenic cytokines within  
7  
8 the liver [1, 36, 37].  
9

10  
11 The mouse model used in this study is ideal to assess the effect of HCV protein  
12  
13 expression on a liver phenomenon. Indeed, these mice specifically express the different  
14  
15 HCV proteins in the liver; however, they are unable to reproduce the complete HCV life  
16  
17 cycle, because the transgene is composed of a cDNA corresponding to the full-length  
18  
19 polyprotein coding region, whereas the 5' and 3' untranslated sequences of the viral  
20  
21 genome necessary for replication of viral RNA are lacking [1].  
22  
23

24  
25 Our findings suggest that HCV protein expression *per se* is not able to induce  
26  
27 fibrosis at a level detectable by common histological and molecular techniques.  
28  
29 Nevertheless, we demonstrate for the first time that hepatic expression of the full-length  
30  
31 HCV ORF *in vivo* is able to enhance fibrosis induced by another fibrogenic agent, a  
32  
33 context similar to chronic human infection where a number of fibrogenic triggers are  
34  
35 present in the liver. Importantly, this effect is independent of the degree of local  
36  
37 inflammation. Our finding that ROS production is significantly increased in HCV  
38  
39 transgenic hepatocytes, both in the absence and presence of CCl<sub>4</sub> treatment, could at  
40  
41 least partly explain that HCV transgenic mice are more susceptible to the development  
42  
43 of liver fibrosis when they are exposed to a 'second hit' by a fibrogenic agent.  
44  
45  
46  
47

48  
49 We show that enhanced liver fibrosis in HCV transgenic animals is associated  
50  
51 with a deregulation of the expression of several matrix remodeling genes. This includes  
52  
53 down-regulation of the expression of MMP13, a protease that specifically degrades  
54  
55 collagen 1, TIMP1, a protein that inhibits MMPs active forms [38], and MMP3, an  
56  
57 activator of pro-MMPs. Thus, HCV transgenic animals seem to be less able to degrade  
58  
59  
60  
61  
62  
63  
64  
65

1  
2  
3  
4 collagen 1, thereby favoring ECM deposition. In addition, the expression of MMP7, a  
5 protease implicated in nerve growth factor-dependent myofibroblast survival [39], was  
6 reduced in CCl<sub>4</sub>-treated HCV mice, whereas a similar trend was found in untreated  
7 transgenic animals, suggesting that HCV protein expression could protect hepatic  
8 myofibroblasts from apoptosis, thus prolonging fibrosis signals.

9  
10  
11 In our study, the enhancement of fibrosis induced by another fibrogenic agent in  
12 transgenic mice expressing the full-length HCV ORF is accompanied by reduced  
13 hepatocyte proliferation, which correlates with the stage of fibrosis. The replacement of  
14 hepatocytes lost from normal hepatic parenchyma is known to occur through replication  
15 of mature hepatocytes [16]. Inhibition of hepatocyte replication by drugs [16], alcohol  
16 [40], steatosis [15] or viral infection [14, 29] promotes the activation of a secondary  
17 replicative pathway involving bipotential HPCs [16]. The activation of HPCs  
18 subsequently leads to the production of both hepatocytes and cholangiocytes, and the  
19 onset of a ductular reaction. The results presented here show that hepatocytes  
20 expressing the full HCV ORF exhibit defective replication after treatment with CCl<sub>4</sub>. Our  
21 acute liver injury experiments suggest that this effect is, at least in part, due to a delayed  
22 entry of hepatocytes into the S-phase of the cell cycle.

23  
24  
25 The defective replication of HCV-expressing hepatocytes leads to the activation  
26 of the HPC pathway and subsequent amplification of the HPC population. In keeping  
27 with this hypothesis, we observed reduced proliferation of mature hepatocytes together  
28 with a marked increase in the number of activated HPCs and a prominent ductular  
29 reaction in CCl<sub>4</sub>-treated FL-N/35 mice. A strong relationship between hepatic fibrosis  
30 severity and the intensity of the ductular reaction has been reported in both rodents and

1  
2  
3  
4 humans [29, 32, 41, 42]. A similar relationship is shown here in the FL-N/35 mouse  
5  
6 strain in the context of HCV protein-induced liver fibrosis [29].  
7  
8

9 In summary, we have shown that transgenic mice expressing the full-length HCV  
10 ORF develop more severe hepatic fibrosis after chronic CCl<sub>4</sub> exposure than  
11 nontransgenic animals. This effect is not linked to local inflammation alterations induced  
12 by HCV proteins. Like during chronic HCV infection in humans, enhanced fibrosis in  
13 HCV transgenic mice is associated with a pronounced ductular reaction, HPC activation  
14 and a concomitant reduction in hepatocyte proliferation that appears to be in part due to  
15 a delayed entry of hepatocytes into the S-phase of the cell cycle. In addition, HCV-  
16 related fibrosis is associated with deregulation of the expression of several matrix  
17 remodeling genes and enhanced ROS production that likely participate in the fibrogenic  
18 process. Overall, our findings in HCV transgenic mice show that expression of the HCV  
19 proteins in hepatocytes contributes to the development of hepatic fibrosis in the  
20 presence of other fibrogenic agents, a situation close to human infection.  
21  
22  
23  
24  
25  
26  
27  
28  
29  
30  
31  
32  
33  
34  
35  
36  
37  
38  
39  
40  
41  
42  
43  
44  
45  
46  
47  
48  
49  
50  
51  
52  
53  
54  
55  
56  
57  
58  
59  
60  
61  
62  
63  
64  
65

**REFERENCES**

- [1] Lerat H, Honda M, Beard MR, Loesch K, Sun J, Yang Y, et al. Steatosis and liver cancer in transgenic mice expressing the structural and nonstructural proteins of hepatitis C virus. *Gastroenterology* 2002;122:352-365.
- [2] Disson O, Haouzi D, Desagher S, Loesch K, Hahne M, Kremer EJ, et al. Impaired clearance of virus-infected hepatocytes in transgenic mice expressing the hepatitis C virus polyprotein. *Gastroenterology* 2004;126:859-872.
- [3] Lerat H, Kammoun HL, Hainault I, Merour E, Higgs MR, Callens C, et al. Hepatitis C virus proteins induce lipogenesis and defective triglyceride secretion in transgenic mice. *J Biol Chem* 2009;284:33466-33474.
- [4] Nishina S, Hino K, Korenaga M, Vecchi C, Pietrangelo A, Mizukami Y, et al. Hepatitis C virus-induced reactive oxygen species raise hepatic iron level in mice by reducing hepcidin transcription. *Gastroenterology* 2008;134:226-238.
- [5] Simonin Y, Disson O, Lerat H, Antoine E, Binaime F, Rosenberg AR, et al. Calpain activation by hepatitis C virus proteins inhibits the extrinsic apoptotic signaling pathway. *Hepatology* 2009;50:1370-1379.
- [6] Higgs MR, Lerat H, Pawlotsky JM. Downregulation of Gadd45beta expression by hepatitis C virus leads to defective cell cycle arrest. *Cancer Res* 2010;70:4901-4911.
- [7] De Leeuw AM, McCarthy SP, Geerts A, Knook DL. Purified rat liver fat-storing cells in culture divide and contain collagen. *Hepatology* 1984;4:392-403.
- [8] Friedman SL. Mechanisms of disease: Mechanisms of hepatic fibrosis and therapeutic implications. *Nat Clin Pract Gastroenterol Hepatol* 2004;1:98-105.

- 1  
2  
3  
4 [9] Friedman SL, Roll FJ. Isolation and culture of hepatic lipocytes, Kupffer cells, and  
5 sinusoidal endothelial cells by density gradient centrifugation with Stractan. *Anal*  
6 *Biochem* 1987;161:207-218.  
7  
8  
9  
10  
11 [10] Kent G, Gay S, Inouye T, Bahu R, Minick OT, Popper H. Vitamin A-containing  
12 lipocytes and formation of type III collagen in liver injury. *Proc Natl Acad Sci USA*  
13 1976;73:3719-3722.  
14  
15  
16  
17  
18 [11] Liang Y, Shilagard T, Xiao SY, Snyder N, Lau D, Cicalese L, et al. Visualizing  
19 hepatitis C virus infections in human liver by two-photon microscopy.  
20 *Gastroenterology* 2009;137:1448-1458.  
21  
22  
23  
24  
25 [12] Roskams TA, Theise ND, Balabaud C, Bhagat G, Bhathal PS, Bioulac-Sage P, et  
26 al. Nomenclature of the finer branches of the biliary tree: canals, ductules, and  
27 ductular reactions in human livers. *Hepatology* 2004;39:1739-1745.  
28  
29  
30  
31  
32 [13] Marshall A, Rushbrook S, Davies SE, Morris LS, Scott IS, Vowler SL, et al.  
33 Relation between hepatocyte G1 arrest, impaired hepatic regeneration, and fibrosis  
34 in chronic hepatitis C virus infection. *Gastroenterology* 2005;128:33-42.  
35  
36  
37  
38 [14] Wagayama H, Shiraki K, Yamanaka T, Sugimoto K, Ito T, Fujikawa K, et al.  
39 p21WAF1/CTP1 expression and hepatitis virus type. *Dig Dis Sci* 2001;46:2074-  
40 2079.  
41  
42  
43  
44  
45  
46  
47 [15] Oben JA, Roskams T, Yang S, Lin H, Sinelli N, Li Z, et al. Sympathetic nervous  
48 system inhibition increases hepatic progenitors and reduces liver injury.  
49 *Hepatology* 2003;38:664-673.  
50  
51  
52  
53 [16] Bissell DM, Roulot D, George J. Transforming growth factor beta and the liver.  
54 *Hepatology* 2001;34:859-867.  
55  
56  
57  
58  
59  
60  
61  
62  
63  
64  
65

- 1  
2  
3  
4 [17] Yang S, Koteish A, Lin H, Huang J, Roskams T, Dawson V, et al. Oval cells  
5  
6 compensate for damage and replicative senescence of mature hepatocytes in mice  
7  
8 with fatty liver disease. *Hepatology* 2004;39:403-411.  
9
- 10  
11 [18] Roskams T, De Vos R, Van Eyken P, Myazaki H, Van Damme B, Desmet V.  
12  
13 Hepatic OV-6 expression in human liver disease and rat experiments: evidence for  
14  
15 hepatic progenitor cells in man. *J Hepatol* 1998;29:455-463.  
16  
17
- 18 [19] Glaser SS, Gaudio E, Miller T, Alvaro D, Alpini G. Cholangiocyte proliferation and  
19  
20 liver fibrosis. *Expert Rev Mol Med* 2009;11:e7.  
21  
22
- 23 [20] Grappone C, Pinzani M, Parola M, Pellegrini G, Caligiuri A, DeFranco R, et al.  
24  
25 Expression of platelet-derived growth factor in newly formed cholangiocytes during  
26  
27 experimental biliary fibrosis in rats. *J Hepatol* 1999;31:100-109.  
28  
29
- 30 [21] Herbst H, Frey A, Heinrichs O, Milani S, Bechstein WO, Neuhaus P, et al.  
31  
32 Heterogeneity of liver cells expressing procollagen types I and IV in vivo.  
33  
34 *Histochem Cell Biol* 1997;107:399-409.  
35  
36
- 37 [22] Malizia G, Brunt EM, Peters MG, Rizzo A, Broekelmann TJ, McDonald JA. Growth  
38  
39 factor and procollagen type I gene expression in human liver disease.  
40  
41 *Gastroenterology* 1995;108:145-156.  
42  
43
- 44 [23] Milani S, Herbst H, Schuppan D, Surrenti C, Riecken EO, Stein H. Cellular  
45  
46 localization of type I, III and IV procollagen gene transcripts in normal and fibrotic  
47  
48 human liver. *Am J Pathol* 1990;137:59-70.  
49  
50
- 51 [24] Paradis V, Dargere D, Vidaud M, de Gouville A-C, Huet S, Martinez V, et al.  
52  
53 Expression of connective tissue growth factor in experimental rat and human liver  
54  
55 fibrosis. *Hepatology* 1999;30:968-976.  
56  
57  
58  
59  
60  
61  
62  
63  
64  
65

- 1  
2  
3  
4 [25] Pinzani M, Milani S, De Franco R, Grappone C, Caligiuri A, Gentilini A, et al.  
5  
6 Endothelin 1 is overexpressed in human cirrhotic liver and exerts multiple effects  
7  
8 on activated hepatic stellate cells. *Gastroenterology* 1996;110:534-548.  
9
- 10  
11 [26] Ramm GA, Nair VG, Bridle KR, Shepherd RW, Crawford DHG. Contribution of  
12  
13 hepatic parenchymal and nonparenchymal cells to hepatic fibrogenesis in biliary  
14  
15 atresia. *Am J Pathol* 1998;153:527-535.  
16  
17
- 18  
19 [27] Sedlaczek N, Jia J-D, Bauer M, Herbst H, Ruehl M, Hahn EG, et al. Proliferating  
20  
21 bile duct epithelial cells are a major source of connective tissue growth factor in rat  
22  
23 biliary fibrosis. *Am J Pathol* 2001;158:1239-1244.  
24  
25
- 26  
27 [28] Wynn TA, Barron L. Macrophages: master regulators of inflammation and fibrosis.  
28  
29 *Semin Liver Dis* 2010;30:245-257.  
30
- 31  
32 [29] Clouston AD, Powell EE, Walsh MJ, Richardson MM, Demetris AJ, Jonsson JR.  
33  
34 Fibrosis correlates with a ductular reaction in hepatitis C: roles of impaired  
35  
36 replication, progenitor cells and steatosis. *Hepatology* 2005;41:809-818.  
37
- 38  
39 [30] Weber LW, Boll M, Stampfl A. Hepatotoxicity and mechanism of action of  
40  
41 haloalkanes: carbon tetrachloride as a toxicological model. *Critical Rev Toxicol*  
42  
43 2003;33:105-136.  
44
- 45  
46 [31] Berres ML, Koenen RR, Rueland A, Zaldivar MM, Heinrichs D, Sahin H, et al.  
47  
48 Antagonism of the chemokine CCL5 ameliorates experimental liver fibrosis in mice.  
49  
50 *J Clin Invest* 2010;120:4129-4140.  
51  
52
- 53  
54 [32] Richardson MM, Jonsson JR, Powell EE, Brunt EM, Neuschwander-Tetri BA,  
55  
56 Bhathal PS, et al. Progressive fibrosis in nonalcoholic steatohepatitis: association  
57  
58 with altered regeneration and a ductular reaction. *Gastroenterology* 2007;133:80-  
59  
60 90.  
61  
62  
63  
64  
65

- 1  
2  
3  
4 [33] Novo E, Parola M. Redox mechanisms in hepatic chronic wound healing and  
5 fibrogenesis. *Fibrogenesis Tissue Repair* 2008;1:5.  
6  
7  
8  
9 [34] Simula MP, De Re V. Hepatitis C virus-induced oxidative stress and mitochondrial  
10 dysfunction: a focus on recent advances in proteomics. *Proteomics Clin Appl*  
11 2010;4:782-793.  
12  
13  
14  
15 [35] Schulze-Krebs A, Preimel D, Popov Y, Bartenschlager R, Lohmann V, Pinzani M,  
16 et al. Hepatitis C virus-replicating hepatocytes induce fibrogenic activation of  
17 hepatic stellate cells. *Gastroenterology* 2005;129:246-258.  
18  
19  
20  
21 [36] Gong G, Waris G, Tanveer R, Siddiqui A. Human hepatitis C virus NS5A protein  
22 alters intracellular calcium levels, induces oxidative stress, and activates STAT-3  
23 and NF-kappa B. *Proc Natl Acad Sci USA* 2001;98:9599-9604.  
24  
25  
26  
27 [37] Moriya K, Nakagawa K, Santa T, Shintani Y, Fujie H, Miyoshi H, et al. Oxidative  
28 stress in the absence of inflammation in a mouse model for hepatitis C virus-  
29 associated hepatocarcinogenesis. *Cancer Res* 2001;61:4365-4370.  
30  
31  
32  
33 [38] Denhardt DT, Feng B, Edwards DR, Cocuzzi ET, Malyankar UM. Tissue inhibitor of  
34 metalloproteinases (TIMP, aka EPA): structure, control of expression and biological  
35 functions. *Pharmacol Ther* 1993;59:329-341.  
36  
37  
38 [39] Kendall TJ, Henedige S, Aucott RL, Hartland SN, Vernon MA, Benyon RC, et al.  
39 p75 neurotrophin receptor signaling regulates hepatic myofibroblast proliferation  
40 and apoptosis in recovery from rodent liver fibrosis. *Hepatology* 2009;49:901-910.  
41  
42  
43 [40] Crary GS, Albrecht JH. Expression of cyclin-dependent kinase inhibitor p21 in  
44 human liver. *Hepatology* 1998;28:738-743.  
45  
46  
47  
48  
49  
50  
51  
52  
53  
54  
55  
56  
57  
58  
59  
60  
61  
62  
63  
64  
65

1  
2  
3  
4 [41] Lowes KN, Brennan BA, Yeoh GC, Olynyk JK. Oval cell numbers in human chronic  
5  
6 liver diseases are directly related to disease severity. Am J Pathol 1999;154:537-  
7  
8 541.  
9

10  
11 [42] Knight B, Akhurst B, Matthews VB, Ruddell RG, Ramm GA, Abraham LJ, et al.  
12  
13 Attenuated liver progenitor (oval) cell and fibrogenic responses to the choline  
14  
15 deficient, ethionine supplemented diet in the BALB/c inbred strain of mice. J  
16  
17 Hepatol 2007;46:134-141.  
18  
19  
20  
21  
22  
23  
24  
25  
26  
27  
28  
29  
30  
31  
32  
33  
34  
35  
36  
37  
38  
39  
40  
41  
42  
43  
44  
45  
46  
47  
48  
49  
50  
51  
52  
53  
54  
55  
56  
57  
58  
59  
60  
61  
62  
63  
64  
65

## FIGURE LEGENDS

**Fig 1. Histological analysis of liver fibrosis in wt and FL-N/35 mice in the absence or presence of chronic CCl<sub>4</sub> exposure. (A)** Representative images of picrosirius red-staining of liver sections from olive-oil and CCl<sub>4</sub>-injected wt and FL-N/35 animals. Scale bars: 100 μm. **(B)** Quantification of picrosirius red-staining from images from various lobes of each liver (6 to 10 images per liver). NS: not significant.

**Fig. 2. mRNA level quantification of genes involved in ECM remodeling in the livers of wt and FL-N/35 mice in the absence or presence of chronic CCl<sub>4</sub> exposure.** mRNA levels of collagens **(A)**, MMPs **(B)** and TIMPs **(C)** were measured by means of qRT-PCR. mRNA levels were normalized to the expression of actin; values are expressed as the percentage of wt animals treated with olive oil (OO).

**Fig. 3. Hepatocyte proliferation in wt and FL-N/35 mice in the absence or presence of chronic CCl<sub>4</sub> exposure. (A)** Representative images of Ki67 immunostaining of liver sections from olive-oil and CCl<sub>4</sub>-treated wt and FL-N/35 animals. Positive Ki67 nuclei are indicated with arrows. Scale bars: 100 μm. **(B)** Quantification of Ki67-positive hepatocytes from various lobes of each liver. Data are expressed as a percentage of total hepatocytes per field. NS: not significant. **(C)** Relationship between hepatocyte proliferation and the extent of CCl<sub>4</sub>-induced ECM deposition in HCV-transgenic mice treated with CCl<sub>4</sub>. Data points represent individual animals. Analysis was performed with 9 animals from 2 independent experiments. **(D)** Relationship between hepatocyte

1  
2  
3  
4 proliferation and the extent of CCl<sub>4</sub>-induced ECM deposition in wt mice treated with  
5  
6 CCl<sub>4</sub>. Data represents 8 animals from 2 independent experiments.  
7  
8  
9

10  
11 **Fig. 4. Ductular reaction in the livers of wt and FL-N/35 mice in the absence or**  
12 **presence of chronic CCl<sub>4</sub> exposure. (A)** CK19-immunostaining of liver sections from  
13  
14 olive oil- and CCl<sub>4</sub>-treated wt and FL-N/35 animals. Open arrows indicate CK19-positive  
15  
16 bile ducts. Black arrows indicate prominent ductules. Arrowheads indicate hepatic  
17  
18 progenitor cells (HPCs). The two lower images show higher magnifications. **(B)**  
19  
20 Quantification of the ductular reaction (CK19-positive bile ducts) in images of CK19  
21  
22 immunostaining of olive oil- and CCl<sub>4</sub>-treated animals. **(C)** Quantification of isolated  
23  
24 HPCs (isolated CK19-positive cells nearby portal tracts) in images of CK19  
25  
26 immunostaining of olive oil- and CCl<sub>4</sub>-treated animals. **(D)** Relationship between the  
27  
28 number of HPCs and the extent of CCl<sub>4</sub>-induced ECM deposition. **(E)** Relationship  
29  
30 between the extent of the ductular reaction and the number of HPCs.  
31  
32  
33  
34  
35  
36  
37  
38  
39  
40

41 **Fig. 5. Hepatocyte DNA synthesis in wt and FL-N/35 mice after acute liver injury**  
42 **caused by high-dose CCl<sub>4</sub> Injection. (A)** Representative photomicrographs of BrdU  
43  
44 immuno-histochemical staining in acutely injured livers from wt and FL-N/35 mice at 0h,  
45  
46 24h, 40h, 48h and 60h post CCl<sub>4</sub> injection. BrdU-positive nuclei are stained in red. Scale  
47  
48 bars = 100 μm. (B) BrdU incorporation at 0h, 24h, 40h, 48h and 60h post CCl<sub>4</sub> injection  
49  
50 in wt and FL-N/35 animals. The number of BrdU-positive hepatocytes was expressed  
51  
52 per μm<sup>2</sup> of tissue area.  
53  
54  
55  
56  
57  
58  
59  
60  
61  
62  
63  
64  
65

1  
2  
3  
4 **Fig. 6. Quantification of ROS levels in the livers of wt and FL-N/35 mice in the**  
5 **absence or presence of chronic CCl<sub>4</sub> exposure. (A) Frozen 10 μm liver sections of**  
6 **olive oil and CCl<sub>4</sub>-treated wt and FL-N/35 mice were stained with DHE and DAPI (insert),**  
7 **and analyzed by fluorescence microscopy. Representative examples are shown. Scale**  
8 **bars = 50 μm. (B) The number of ROS-positive hepatocytes was measured, and is**  
9 **shown as the percentage of ROS-positive cells as described in the Material and**  
10 **Methods section.**  
11  
12  
13  
14  
15  
16  
17  
18  
19  
20  
21  
22  
23  
24  
25  
26  
27  
28  
29  
30  
31  
32  
33  
34  
35  
36  
37  
38  
39  
40  
41  
42  
43  
44  
45  
46  
47  
48  
49  
50  
51  
52  
53  
54  
55  
56  
57  
58  
59  
60  
61  
62  
63  
64  
65

**Table 1.** Age, body and liver weights and ALT/AST levels in wt and FL-N/35 mice chronically exposed or not to CCl<sub>4</sub>. Mean±SEM values are shown. NS: not significant.

	Olive oil		p	CCl <sub>4</sub>		p
	wt (n=15)	FL-N/35 (n=15)		wt (n=13)	FL-N/35 (n=17)	
Age (month)	8-10	8-10		8-10	8-10	
Body weight (g)	33.7±0.8	33.9±1.2	NS	30.0±3.5	31.3±3.9	NS
Liver weight (g)	1.5±0.04	1.5±0.09	NS	1.5±0.3	1.4±0.4	NS
ALT (IU/mL)	42±12.6	46±22.8	NS	2570.5±479.5	1654.8±316.9	NS
AST (IU/mL)	63.2±20.7	81.6±32.8	NS	1532.5±319.7	921±170	NS

Figures  
**Figure 1A**

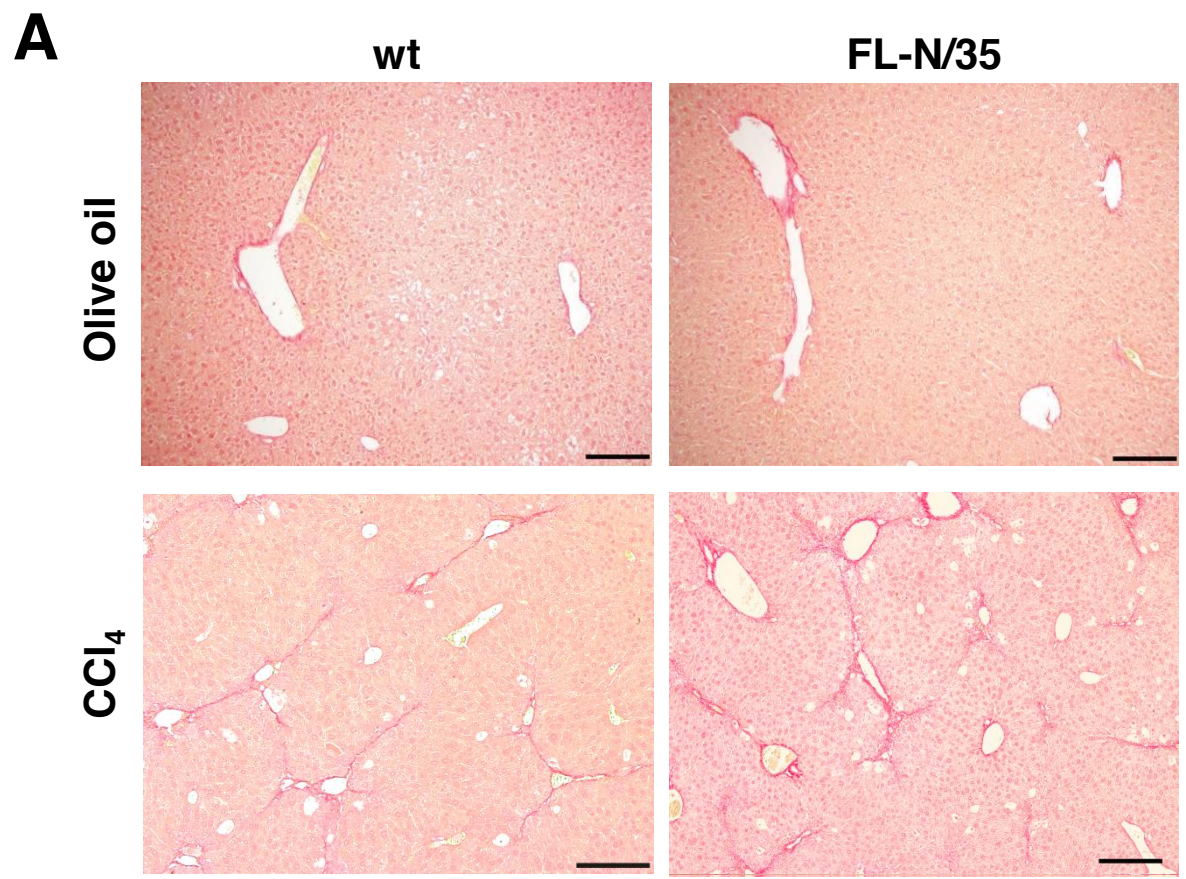
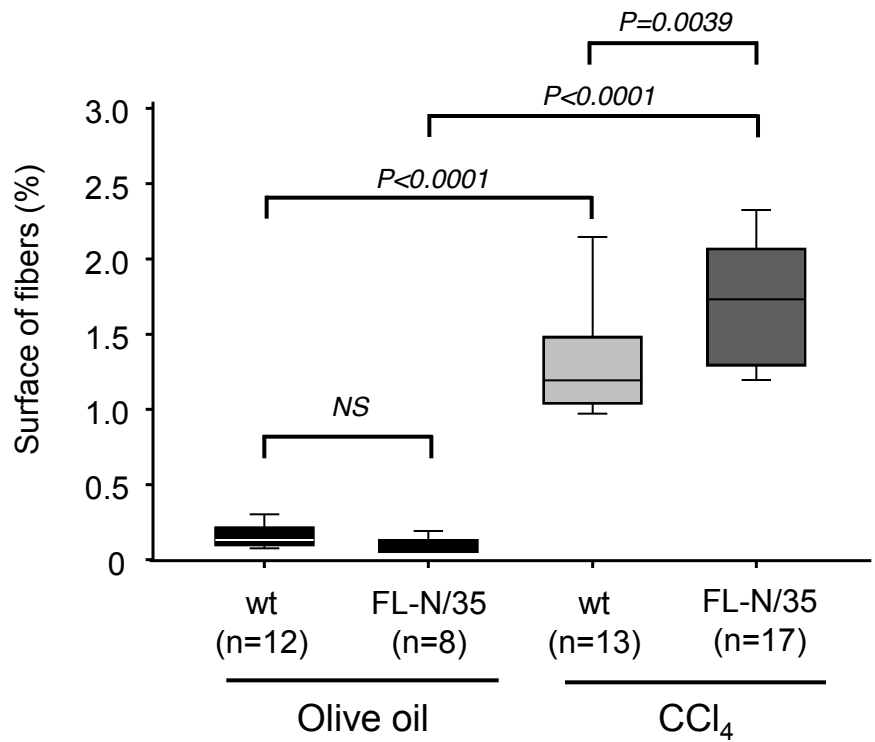


Figure 1B

**B**



**Figure 2A**

**A**

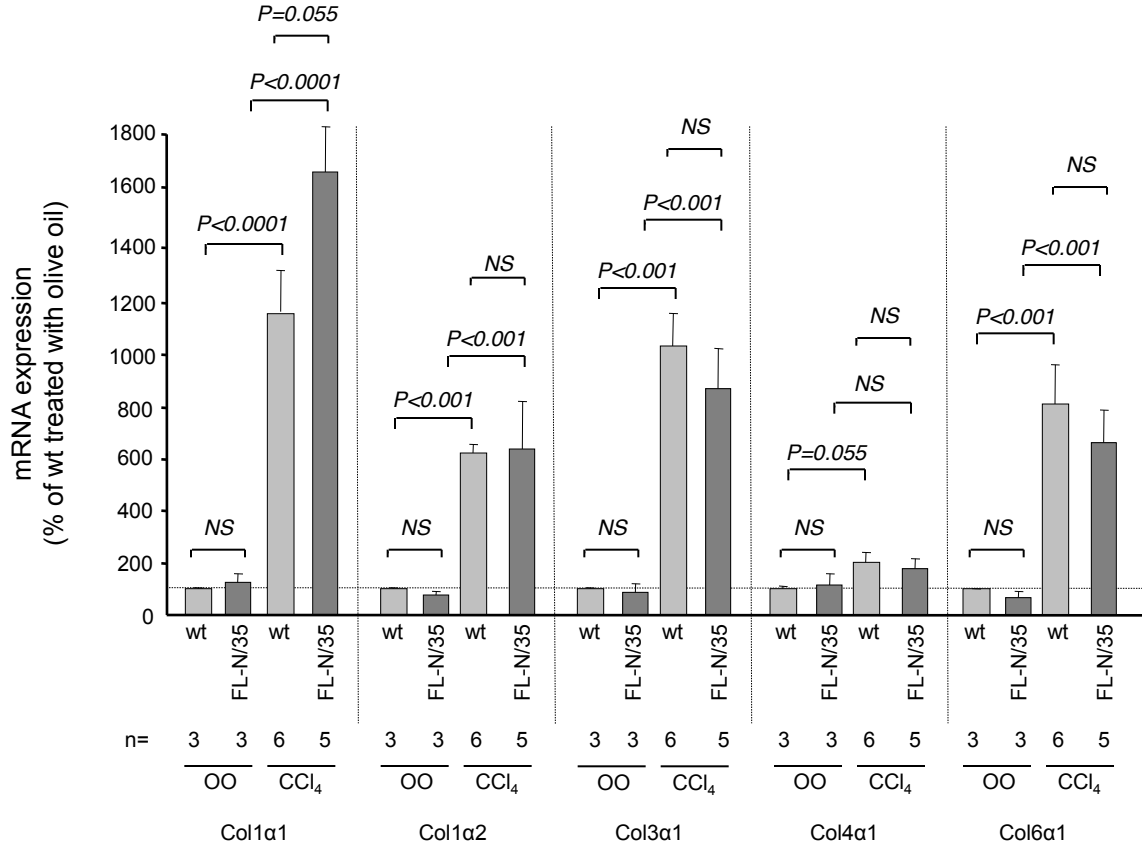


**Figure 2B**

**B**

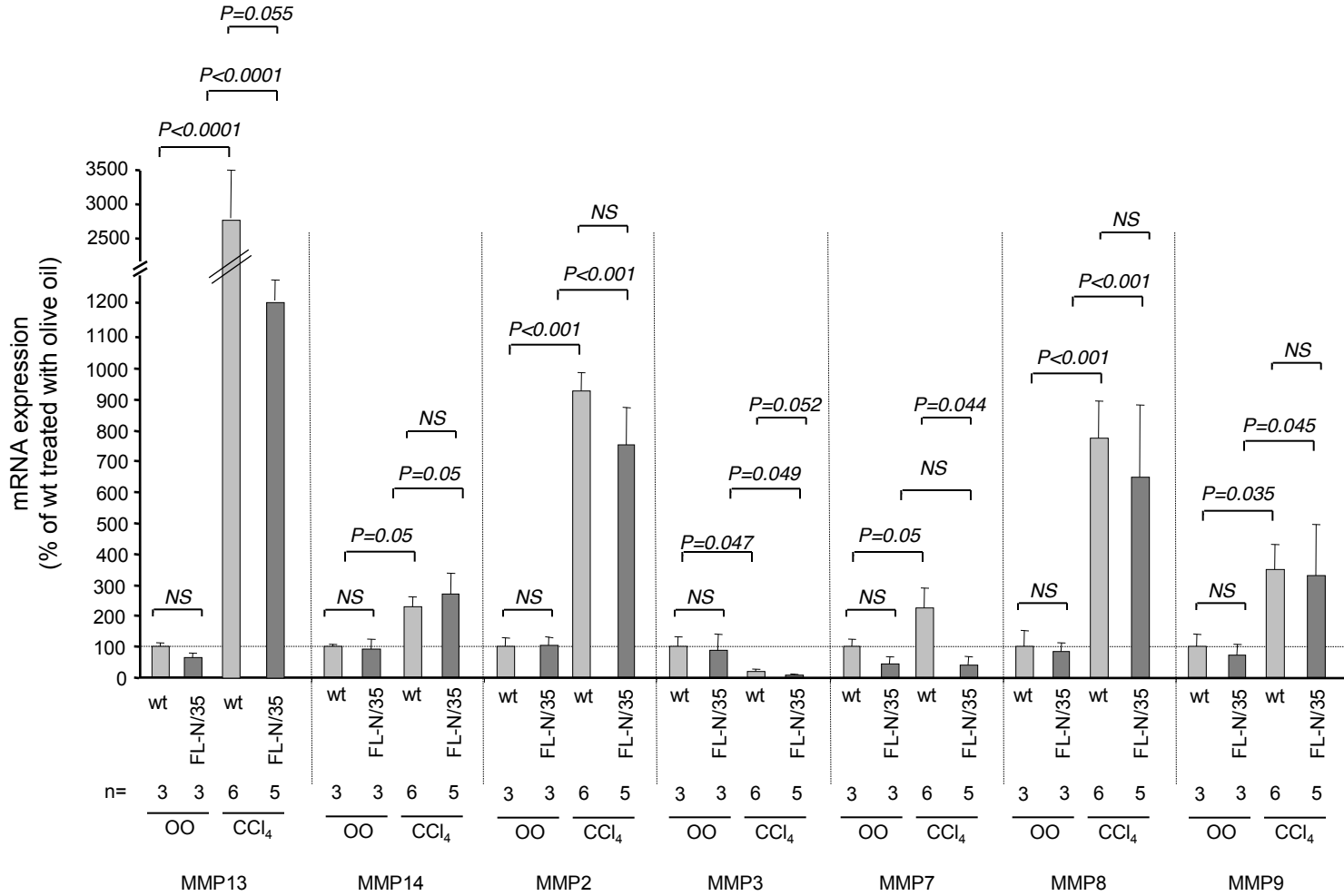


Figure 2C

C

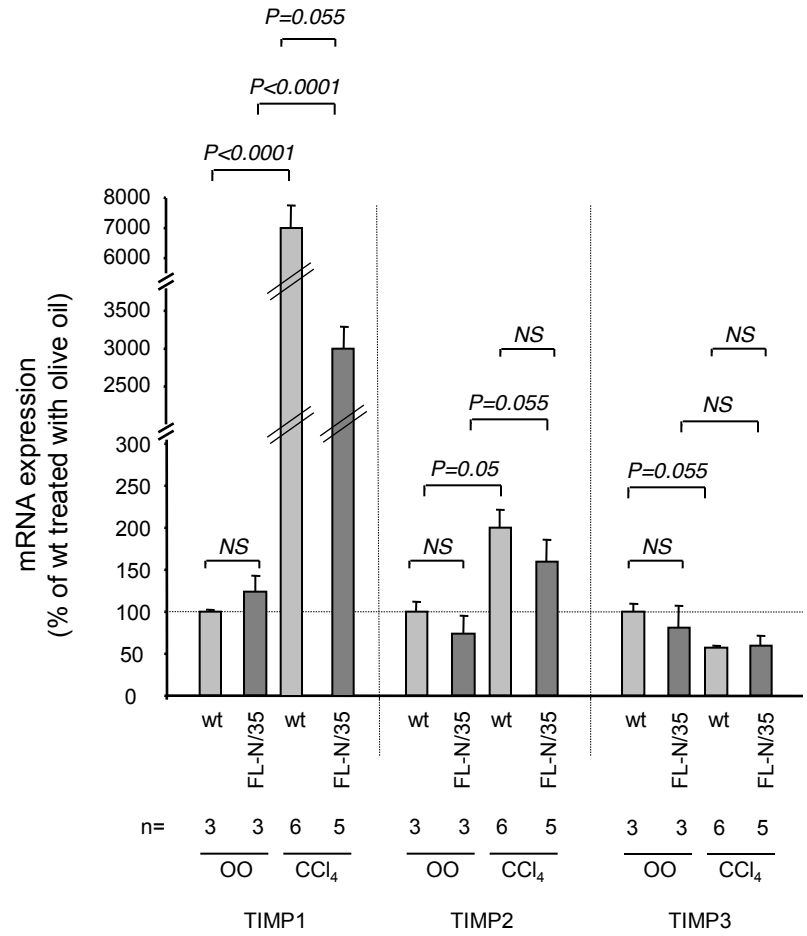


Figure 3A

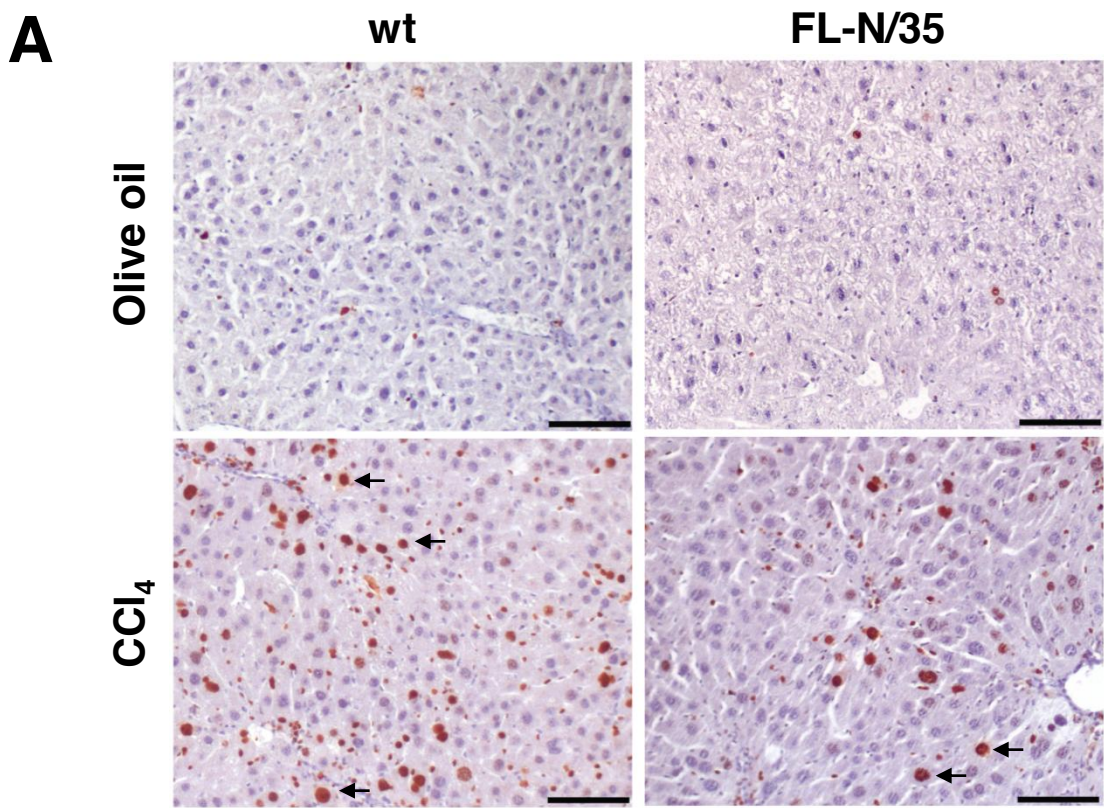


Figure 3B

**B**

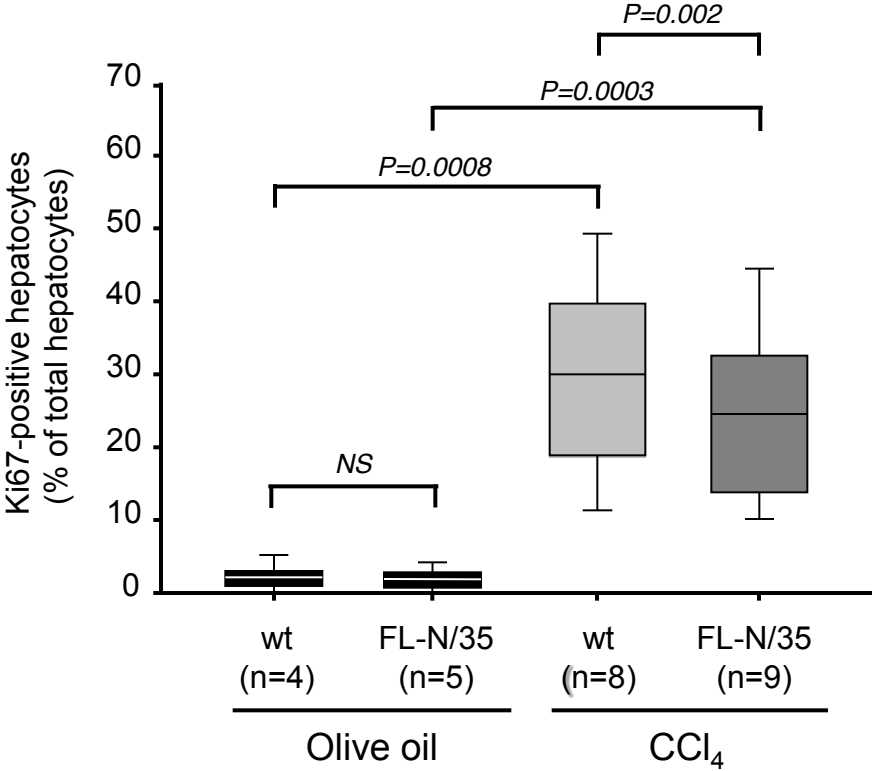


Figure 3C

C

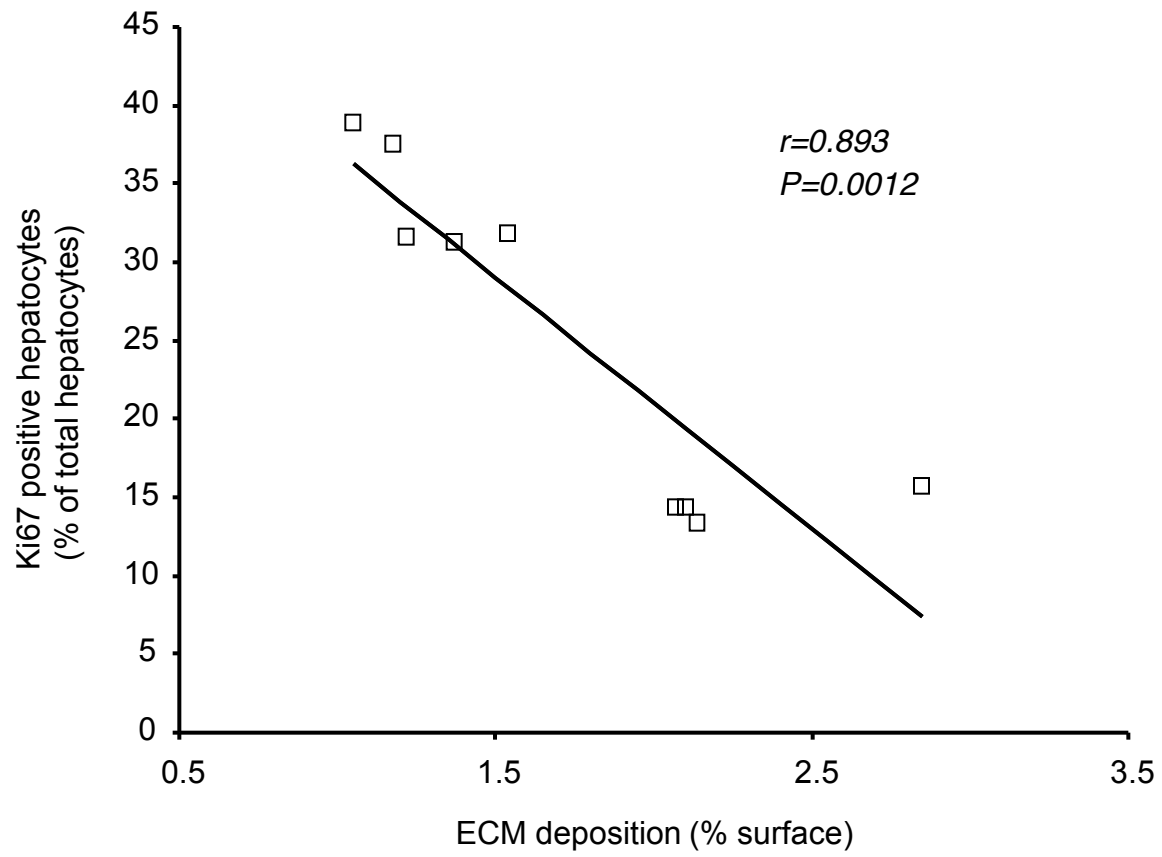


Figure 3D

**D**

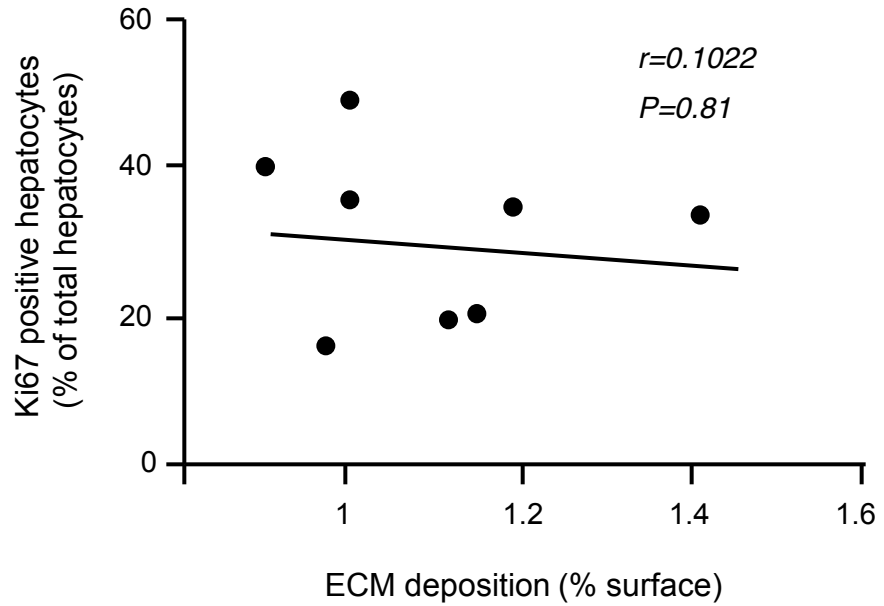


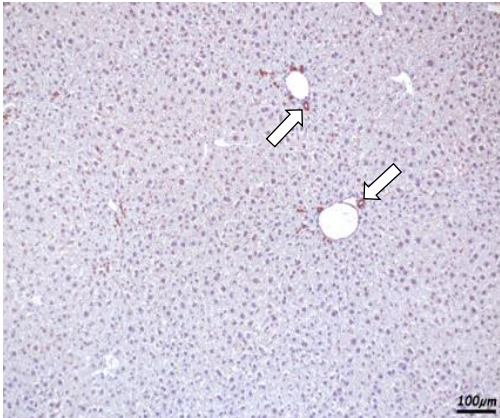
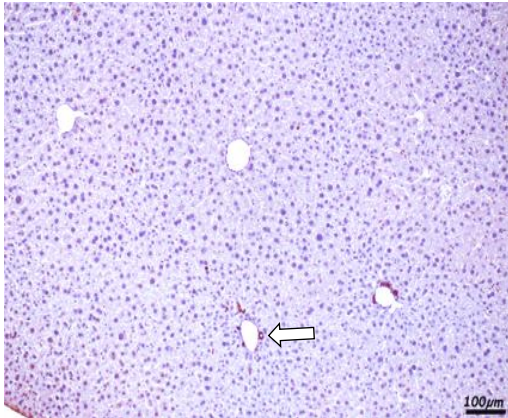
Figure 4A

**A**

**wt**

**FL-N/35**

**Olive oil**



**CCl<sub>4</sub>**

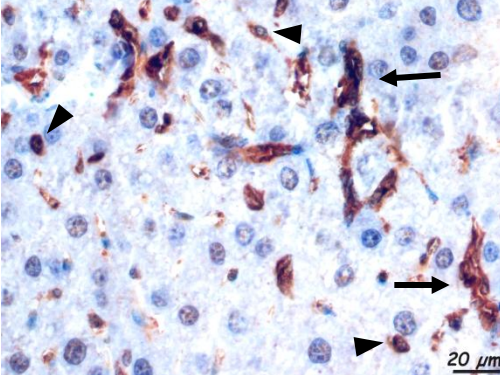
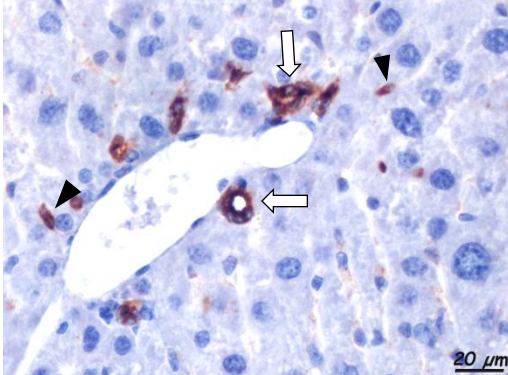
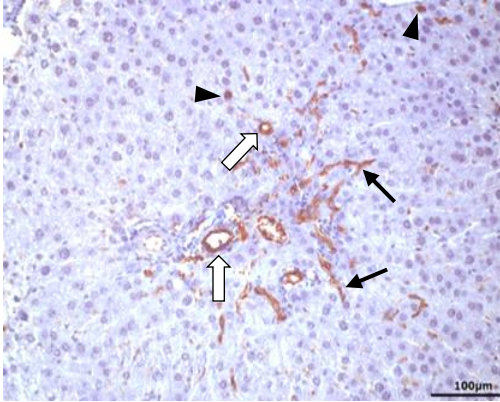
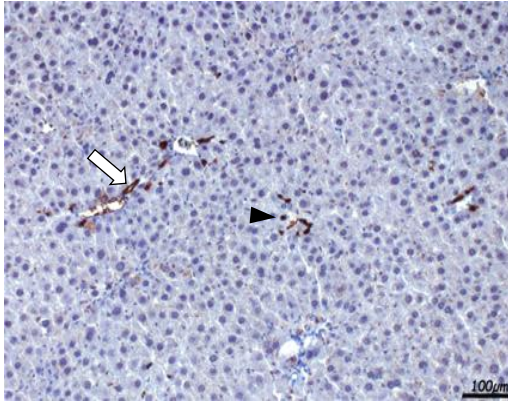


Figure 4B

**B**

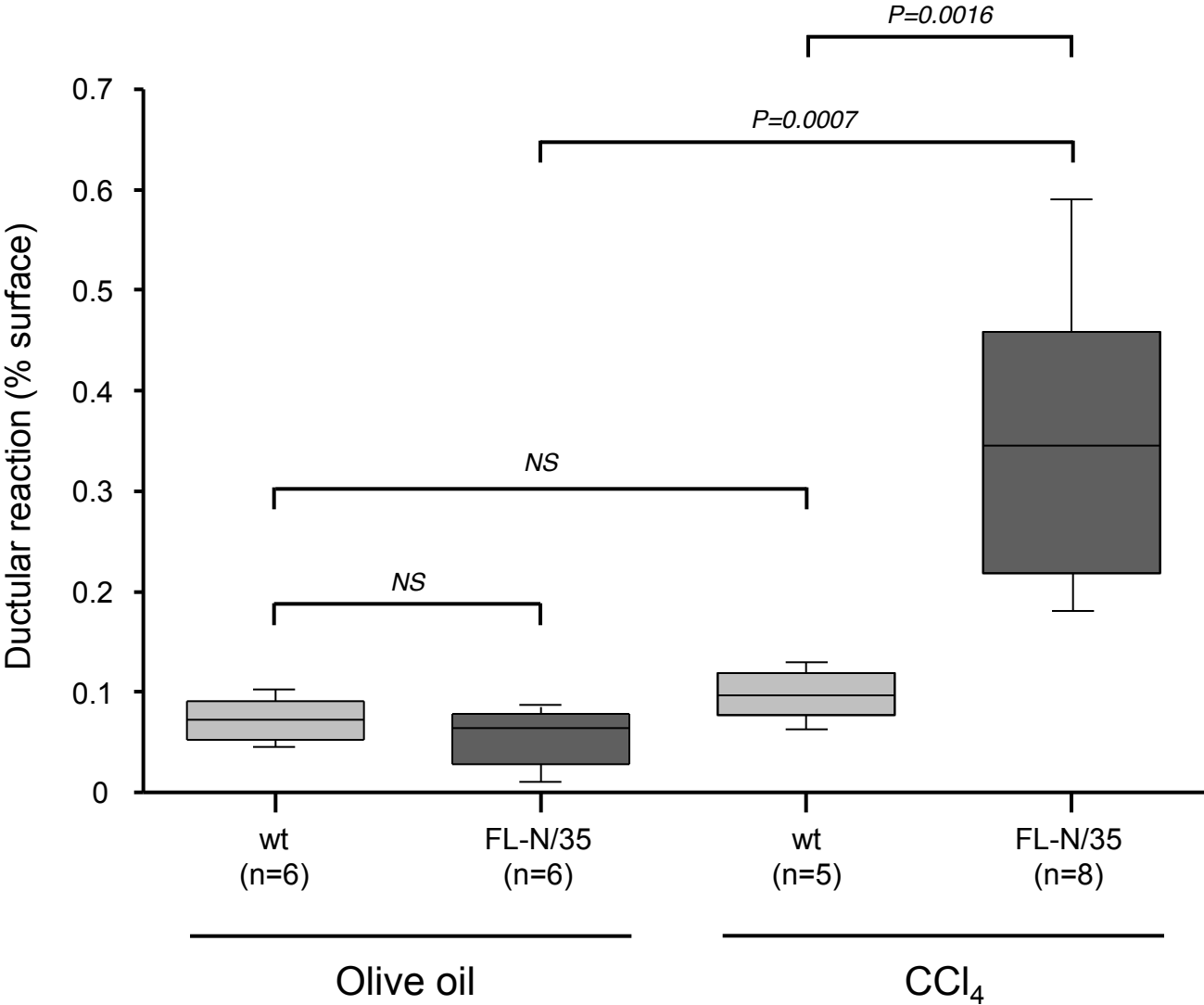


Figure 4C

C

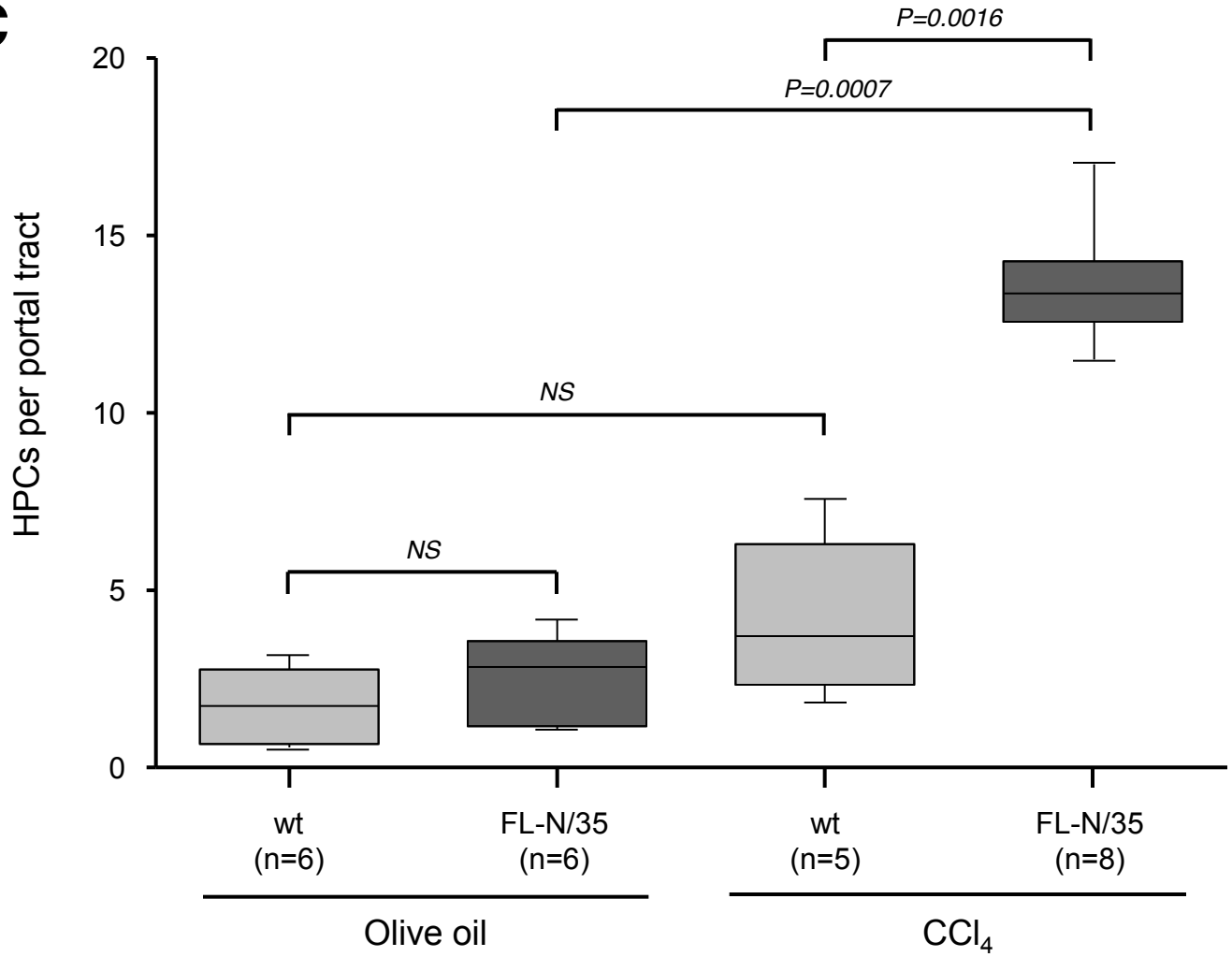


Figure 4D

D

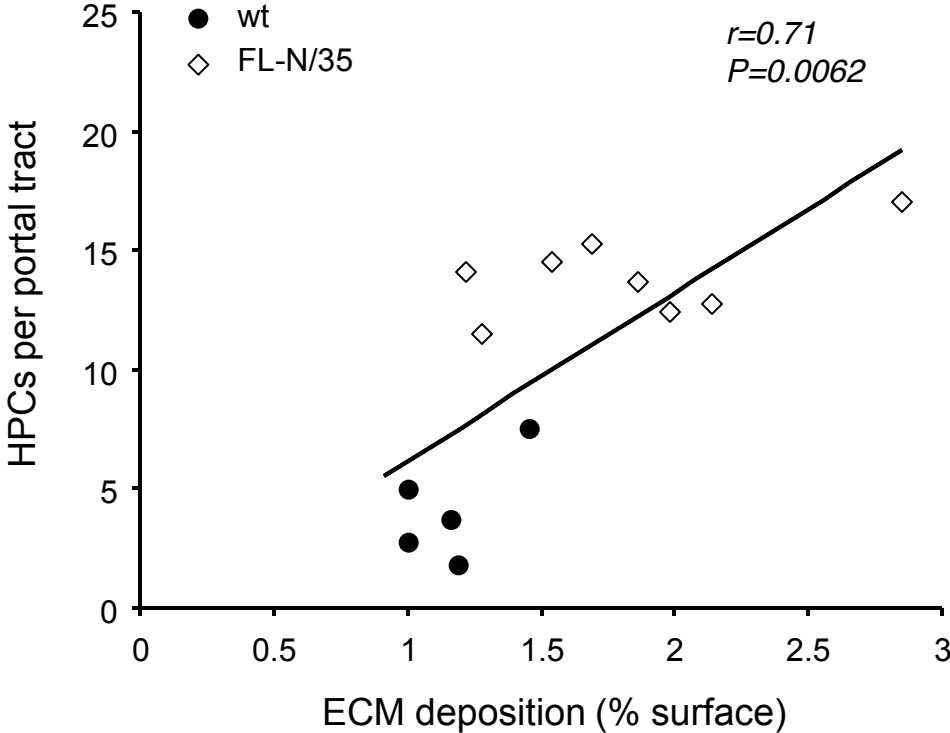


Figure 4E

**E**

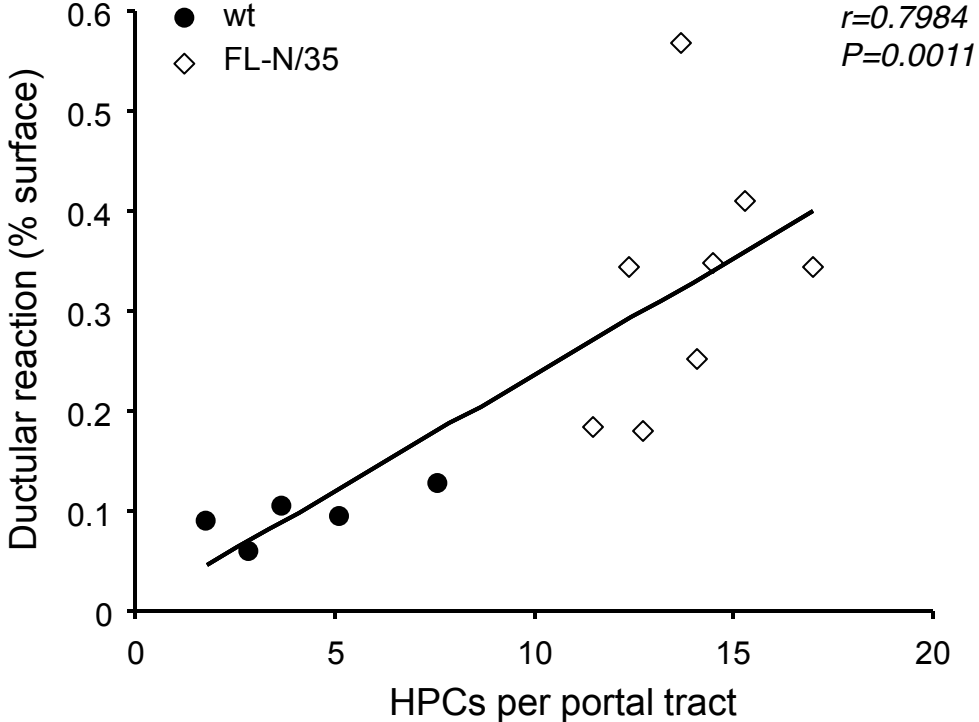


Figure 5A

**A**

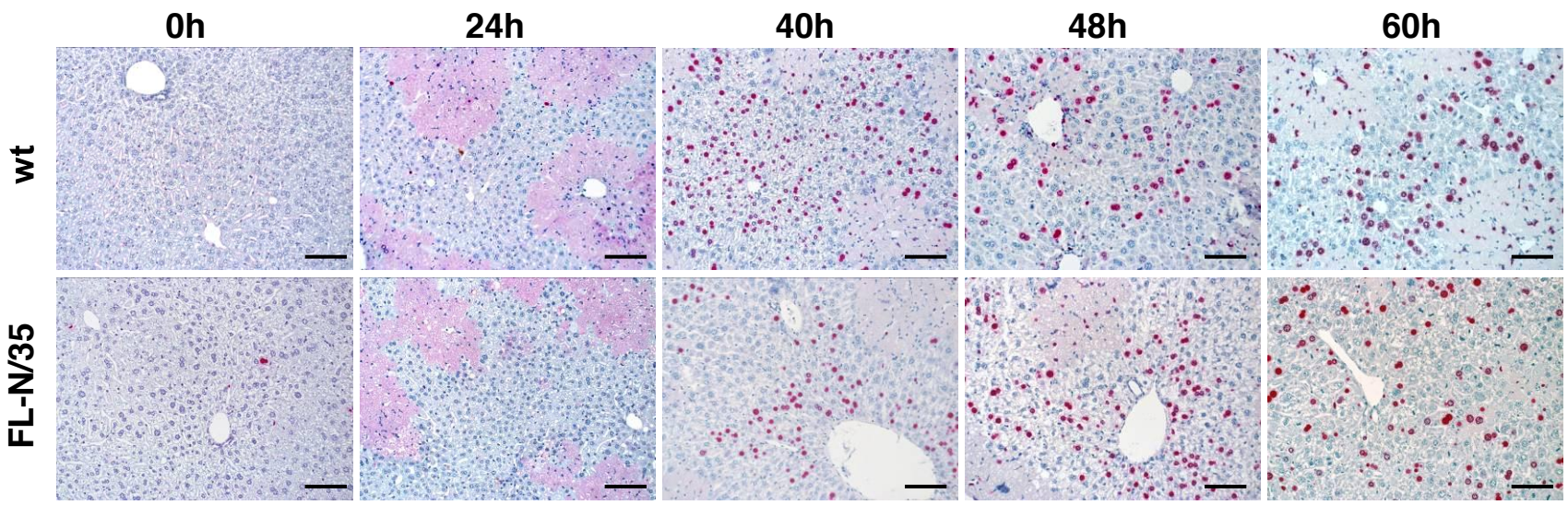


Figure 5B

**B**

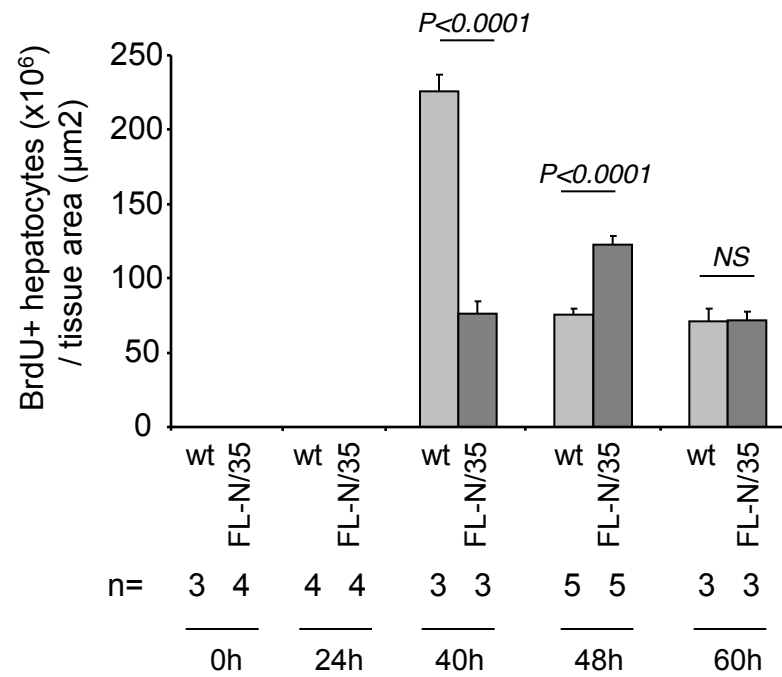


Figure 6A

**A**

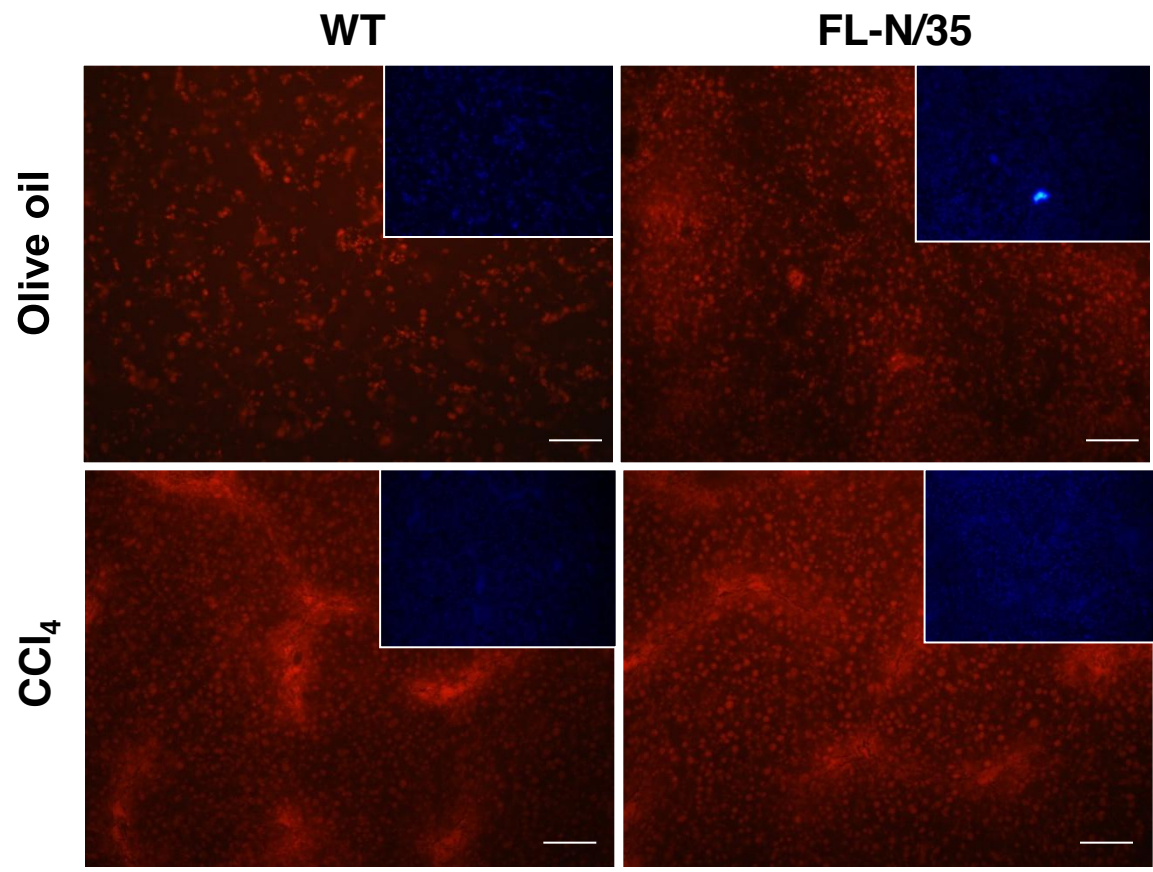
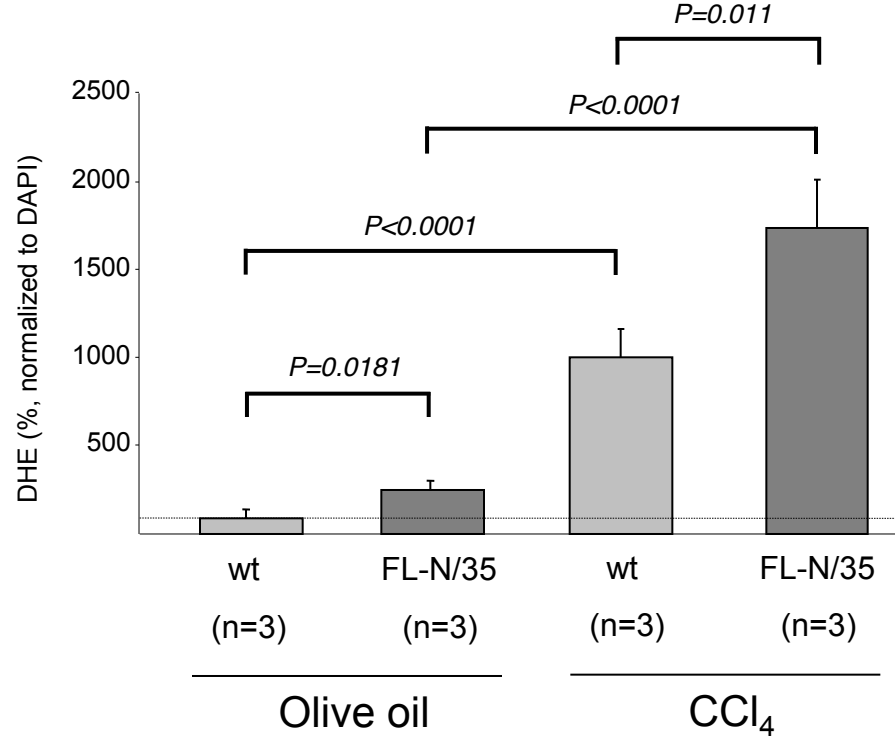


Figure 6B

**B**



**Supplementary Materials and Methods**

[Click here to download Supplementary material: Supplementary Materials and Methods.doc](#)

## Supplementary Figures

[Click here to download Supplementary material: Supplementary Figures.ppt](#)